

1 **Influence of Clinker Melt Composition on Reactions at the Surface of Alite**
2 **Crystals during Cooling**

3

4 Matthias Böhm, VDZ Technology gGmbH, Toulouser Allee 71, 40476 Duesseldorf,
5 matthias.boehm@vdz-online.de, +49 211 45 78 293

6

7 Aneta Knöpfelmacher, VDZ Technology gGmbH, Toulouser Allee 71, 40476
8 Duesseldorf, aneta.knoepfelmacher@vdz-online.de, +49 211 45 78 386

9

10 **ABSTRACT**

11 Microstructural features of industrial Portland cement clinker samples are presented
12 to illustrate the influence of the clinker melt chemistry on the reactions taking place
13 on the surfaces of alite crystals during cooling at high temperatures. While clinker
14 melts rich in Al_2O_3 are usually undersaturated with respect to CaO, leading to corro-
15 sion of alite crystals and formation of secondary belite, clinker melts rich in Fe_2O_3 are
16 oversaturated with respect to CaO. This leads to a final growth step of alite during
17 cooling, as long as the clinker temperature is still in the stability field of alite
18 ($> 1250\text{ }^\circ\text{C}$). In the first case, the microstructural features of the alite surface permits
19 conclusions on the length of the precooling zone in the rotary kiln, which is closely
20 connected to the flame shape. In the latter case, such conclusions cannot be drawn.

21

22 **KEYWORDS**

23 Alite, alumina ratio, clinker melt, cooling, flame shape

24

25 **INTRODUCTION**

26 The increased substitution of conventional fuels by alternative fuels in the production
27 process of Portland cement clinker is essential for the decarbonisation of cement and
28 concrete¹. The use of increased amounts of alternative fuels on the main burner of
29 the rotary kiln often requires modern multi-channel burners, which allow the control of
30 the flame shape. This is necessary because some alternative fuel types like fluff can
31 contain particle types with different burning behaviour due to variations in chemical
32 composition, moisture content, size, specific surface or ignition temperature². In order
33 to optimise the burner settings, information on the flame shape with given burner set-
34 tings are important.

35 A widespread method to evaluate the rotary kiln flame characteristics is flame ther-
36 mography with a pyrometric camera². However, under some circumstances like high
37 dust contents the applicability of the method is restricted³ or such a system is not
38 available. Therefore other sources of information on the flame shape can be very
39 useful.

40 For clinkers with alumina ratios ($AR = Al_2O_3/Fe_2O_3$) > 1.4 the interpretation of the
41 constitution of alite surfaces with clinker microscopy can contribute such information.
42 However, observations on several technical clinker samples presented here show
43 that for clinkers with $AR < 1.4$ the reactions occurring during cooling lead to different
44 microstructural features that are currently not assignable to certain flame characteris-
45 tics.

46

47 **MATERIALS AND METHODS**

48 All observations presented in this paper were made on technical clinker samples. The
49 materials were sampled by the respective producer. The clinker samples were
50 crushed in a jaw crusher and fractions of 2 to 4 mm were retrieved as subsamples
51 from the crushed material by sieving. The subsamples were embedded in epoxy res-

52 in under vacuum. After curing, polished sections of the embedded samples were pro-
53 duced. The sections were successively etched with an alcoholic dimethyl ammonium
54 citrate (DAC) solution and with a KOH solution. The etched sections were studied
55 with an optical microscope under reflected light.

56 The calculation of the alumina ratios (AR) of the samples was based on their chemi-
57 cal compositions, which were analysed with X-ray fluorescence analysis (XRF) on
58 fused beads.

59

60 **REACTIONS IN CLINKER UPON COOLING**

61 The shape of the main burner flame in a rotary kiln is an important factor controlling
62 the length of the precooling zone, i.e. the last section of the rotary kiln, where the
63 clinker temperature is already decreasing from the temperature in the sintering zone
64 (ca. 1450 °C) due to contact with cooler air entering the kiln from the clinker cooler
65 (secondary air)⁴. A short flame leads to a short precooling zone, while a long flame
66 leads to a long precooling zone.

67 The clinker usually reaches temperatures of ca. 1200 – 1250 °C in the precooling
68 zone before falling into the clinker cooler⁴, which is around or below the lower ther-
69 modynamic stability limit of alite⁵ and the formation/crystallisation temperature of the
70 clinker melt⁶. Due to the fast cooling of modern technical clinkers, alite is almost al-
71 ways preserved in a metastable state, without signs for decomposition⁷. Microstruc-
72 tural features of the surfaces of alite crystals are therefore only influenced by reac-
73 tions with the clinker melt, which partly or fully crystallises in the precooling zone. The
74 clinker melt mostly crystallises to C₃A and C₄AF, with minor amounts of periclase and
75 calcium silicates.

76

77 **Clinker with AR > 1.4**

78 If the clinker melt is rich in Al_2O_3 , which is usually the case for clinkers with $\text{AR} > 1.4$,
79 its crystallisation requires more CaO than it contains, i.e. it is undersaturated with
80 respect to CaO. As a result the melt primarily reacts with alite crystals and retrieves
81 CaO from their surfaces^{4,7,8}. This effect increases with increasing Al_2O_3 contents^{4,8}.
82 The reaction leads to irregular, corroded alite crystal surfaces and, due to the CaO-
83 extraction, to the formation of a rim of secondary belite surrounding the alite crystal. If
84 the precooling zone is short, the system is cooled fast below ~ 1200 °C and the fine
85 grained rims of secondary belite as well as the corroded alite surfaces are pre-
86 served^{4,8} (Figure 1A). In a longer precooling zone the clinker is exposed to high tem-
87 peratures for a longer period of time. This allows coarsening of the secondary belite
88 by collective crystallisation. The belite rings transform into several separate belite
89 crystals around alite. Simultaneously the rough surfaces of alite crystals recrystallise
90 and smoothen (Figure 1B).

91

92 **Clinker with $\text{AR} < 1.4$**

93 Clinker samples rich in Fe_2O_3 often do not show systematic signs of alite corrosion.
94 On the contrary, microstructural features observed in several technical clinker sam-
95 ples with $\text{AR} < 1.4$ indicate a short final stage of alite growth, most probably occurring
96 during cooling, but at temperatures above the lower thermodynamic stability limit of
97 alite, i.e. in the precooling zone. Figure 2 shows four situations observed in clinker
98 samples with $\text{AR} < 1.4$.

99 Figure 2A shows alite crystals with uncorroded surfaces and with protrusions (“nos-
100 es”). These noses seem to expand only the $\{0001\}$ crystal faces acc.⁹, i.e. the basal
101 pinacoids, of the alite crystals and can be explained by lateral growth of these faces.
102 The small size of the “noses” and the growth of the outermost and therefore youngest

103 crystal faces show that the growth step was short and occurred at the very end of the
104 residence time of the material in the alite stability field.

105 Figure 2B shows alite crystals with signs of zonation, visible due to different etching
106 colours. The outer alite zones are interrupted by belite crystals. The combination of a
107 strongly jagged alite surface with distinct, large belite crystals is very untypical for the
108 reactions described above (alite corrosion, secondary belite formation and recrystalli-
109 sation). Therefore a different formation mechanism is more plausible. The common
110 starting point of several belite crystals on the same alite zone indicates that the belite
111 crystals grew on a former alite surface. The irregular shape of the belite crystals indi-
112 cate that the crystals were partly converted into alite, probably while they were over-
113 grown by the outer and therefore younger alite zones, which formed in a final stage
114 of growth.

115 Figure 2C shows a cluster of belite crystals many of which have small crystals
116 ("crusts") of alite on their surfaces. Since belite crystals recrystallise and grow in the
117 sintering zone of the kiln, the formation of these "crusts" can be assigned to the kiln
118 section following the sintering zone, i.e. the precooling zone.

119 Figure 2D shows a cluster of belite crystals. The cluster has a circular center mostly
120 consisting of C_4AF with interspersed lath shaped alite crystals. This phenomenon has
121 been described for Fe_2O_3 -rich clinker before and was interpreted as alite crystallised
122 directly from the melt phase during cooling⁸. It shows that the melt contained all con-
123 stituents for alite formation, including a high amount of CaO. Very similar alite crys-
124 tals formed on the surface of belite crystals, probably at least partly converting belite
125 into alite. Like the example shown in Figure 2C, the formation of alite on the surface
126 of belite crystals indicates that this reaction occurred at the very end of the clinker's
127 residence time at high temperatures.

128 The final short growth step of alite in the precooling zone, as illustrated by the four
129 situations in Figure 2, can be explained by an oversaturation of the Fe_2O_3 -rich clinker
130 melt with respect to CaO. When the melt starts to crystallise, the surplus CaO, which
131 is not needed for the crystallisation of C_4AF and C_3A , reacts with belite to form alite.
132 The situation in Figure 2D shows that the CaO can even directly form alite during
133 cooling, together with SiO_2 dissolved in the clinker melt.

134

135 **CONCLUSIONS**

136 It can be concluded from the observations shown above that the constitution of alite
137 surfaces can presently only serve as a direct indicator for the length of the precooling
138 zone and an indirect indicator for the flame shape, if the alumina ratio (AR) of the cor-
139 responding clinker is above 1.4. Otherwise alite crystals are not corroded, but instead
140 grow in the precooling zone. However, it should be kept in mind that, due to local in-
141 homogeneities in the distribution of Al_2O_3 and Fe_2O_3 or other influences, features of
142 alite corrosion and of alite growth can occur in the same clinker sample.

143 It remains unclear, which of the shown manifestations of alite growth occurs under
144 which circumstances. Additionally it is unclear, if or how different lengths of the pre-
145 cooling zone influence the microstructural features of the final growth step of alite in
146 clinkers with an AR below 1.4. Further systematic observations of Fe_2O_3 -rich clinkers
147 should provide this information.

148

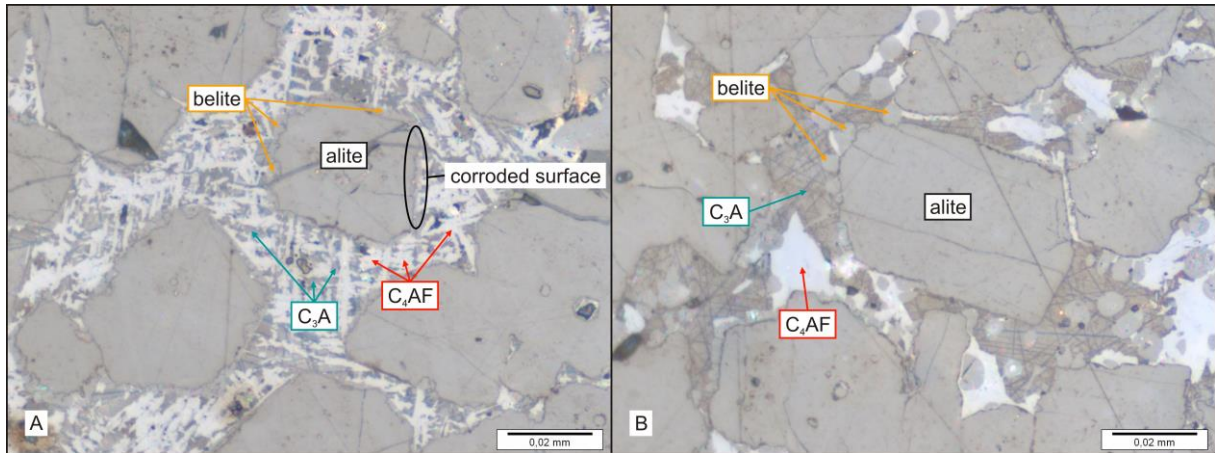
149 **REFERENCES**

150 1. Schneider, M., Romer, M., Tschudin, M., Bolio, H. (2011) Sustainable cement pro-
151 duction – present and future. Cement and Concrete Research 41, 642 – 650.

- 152 2. Wirthwein, R., Emberger, B. (2010) Burners for alternative fuels utilisation - optimi-
153 sation of kiln firing systems for advanced alternative fuel co-firing. Cement Interna-
154 tional 8 (4), 42 – 46.
- 155 3. Pedersen, M. N., Nielsen, M., Clausen, S., Jensen, P. A., Jensen, L. S., Dam-
156 Johansen, K. (2017) Imaging of Flames in Cement Kilns To Study the Influence of
157 Different Fuel Types. Energy & Fuels 31 (10), 11424 – 11438.
- 158 4. Hoenig, V., Sylla, H.-M. (1998) Industrial clinker cooling with due regard to the ce-
159 ment properties. ZKG International 51 (6), 318 – 333.
- 160 5. Wolter, A. (1982), Zur Bildung und Stabilität von Tricalciumsilikat und Aliten, For-
161 schungsberichte des Landes Nordrhein-Westfalen, No. 3092, Fachgruppe
162 Bau/Steine/Erden, Westdeutscher Verlag GmbH, Opladen
- 163 6. de la Torre, A. G., Morsli, K., Zahir, M., Aranda, M.A. G. (2007) In situ synchrotron
164 powder diffraction study of active belite clinkers. Journal of Applied Crystallography
165 40, 999 – 1007.
- 166 7. Böhm, M., Knöpfelmacher, A., Pierkes, R. (2017) Alite decomposition vs. alite cor-
167 rosion. Proceedings of the 16th Euroseminar on Microscopy Applied to Building Ma-
168 terials, Les Diablerets
- 169 8. Verein Deutscher Zementwerke e.V. (ed.) (1965) Mikroskopie des Zementklinkers
170 – Bilderatlas. Beton-Verlag GmbH, Düsseldorf
- 171 9. Yamaguchi, G., Ono, Y. (1966) Mikroskopische Untersuchungen am Alit des Port-
172 landzementklinkers. Zement-Kalk-Gips (9), 390 – 394.

173

174



175

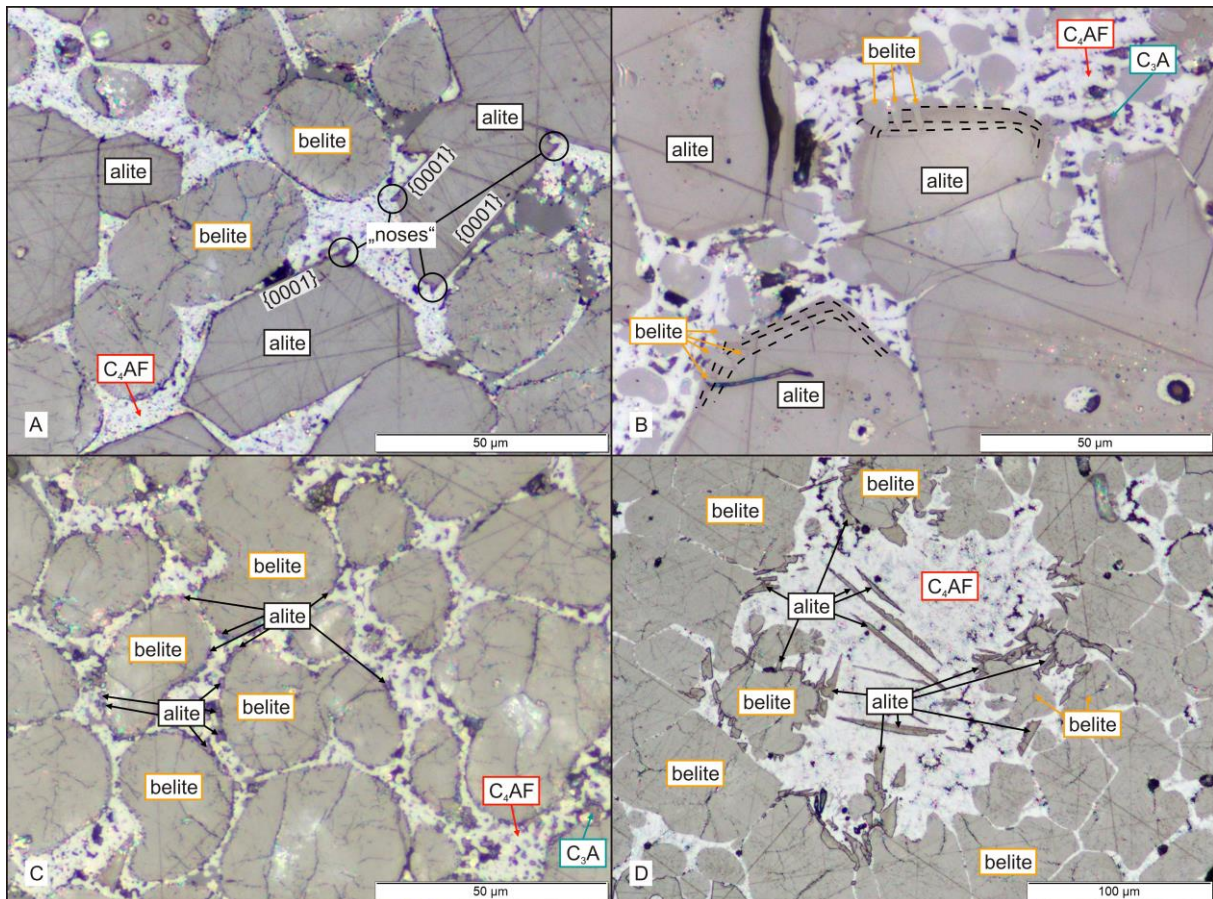
176 Figure 1: A) alite crystals with corroded surfaces surrounded by thin rims of second-

177 ary belite, fine to intermediately fine crystals of C_3A and C_4AF ; B) alite crystals with

178 partly corroded, partly smooth surface surrounded by single crystals of secondary

179 belite, coarse crystals of C_3A and C_4AF ; both figures taken from ⁷

180



181

182 Figure 2: A) alite crystals with uncorroded surfaces, partly with “noses” due to lateral

183 growth of {0001} crystal faces, fine crystals of C_4AF ; B) zoned alite crystals with un-

184 corroded surfaces overgrowing belite crystals, dashed lines mark visible zone

185 boundaries, intermediately fine crystals of C_4AF and C_3A ; C) “crusts” of small alite

186 crystals on the surfaces of belite crystals, fine to intermediately fine crystals of C_4AF

187 and C_3A ; D) cluster of belite crystals, circular center mostly consisting of C_4AF and

188 lath shaped alite crystals formed on the surface of belite crystals or crystallised di-

189 rectly from the melt phase

190

191